Received: 25 May 2023 | Revised: 20 September 2023 | Accepted: 26 October 2023

DOI: 10.1002/joc.8302

RESEARCH ARTICLE

International Journal of Climatology RMetS

Temperature variation in the South Orkney Islands, maritime Antarctic

Hua Lu | **Steve Cowell** | **John King** | **Andrew Orr** | **Tony Phillips** | **Emilia Dobb** | **Jonathan Xue** | **Sabina Kucieba** | **Guy Phillips** | **Gareth Marshall**

British Antarctic Survey, Cambridge, United Kingdom

Correspondence
Hua Lu, British Antarctic Survey, High Cross, Madingley Road, Cambridge CB3 0ET, UK.
Email: hlu@bas.ac.uk

Funding information
British Antarctic Survey; Natural Environment Research Council, Grant/Award Number: NE/X009319/1; European Union's Horizon 2020, Grant/Award Number: 101003590

Abstract

Meteorological records at Signy Station in the South Orkney Islands (SOIs) have recently been digitized to cover the period of 1947–1995. This study compares the newly available near-surface air temperatures at Signy with those from a nearby station, Orcadas and with reanalysis datasets to provide a more comprehensive picture of the weather and climate variability in the SOIs. Temperatures from both stations show a higher degree of variability in winter than summer, but the variability differs in terms of its relationship to the dominant wind directions and sea ice influences. The two stations differ markedly in terms of their respective warm temperature events, largely due to orography-induced föhn winds at Signy Station as northwesterlies flow over Coronation Island. ERA5 reproduces the monthly to annual averages exceedingly well but underestimates both cold and warm tails of station temperatures. Temperature trends in the SOIs are also considered in terms of changes in large-scale circulation and the sea surface temperature over the Brazil-Falkland Confluence. However, caution is required in interpreting the long-term temperature trends estimated from reanalysis data as most of the reanalyses show a cold bias before 1979, which is most likely caused by misrepresentation of the sea ice.

KEYWORDS

antarctic islands, regional climate variability, synoptic observations, temparature variation

1 | INTRODUCTION

The South Orkney Islands (SOIs), a group of maritime Antarctic islands in the Atlantic sector of the Southern Ocean at the confluence of the Weddell Sea and the Scotia Sea (Figure 1), have rich and diverse terrestrial ecosystems that are impacted by climate change (Cannone et al., 2022; Rootes, 1988; Royles et al., 2012). The surrounding shelf waters are also nutrition-rich, which is vital in terms of Southern Ocean biodiversity (Meredith et al., 2015; Moline et al., 2004). Maritime Antarctic ecosystems and biodiversity are highly sensitive to temperature and other environmental change (Ballerini et al., 2014; Convey & Peck, 2019). It is thus vital to understand temperature variation and trends in the SOIs.

The regional drivers of temperature variation over the SOIs are the prevailing westerlies and the intense cyclonic systems associated with the Southern Ocean

storm tracks (Hoskins & Hodges, 2005). These weather systems are influenced by the Southern Annular Mode (Marshall, 2003; Marshall & Thompson, 2016) as well as tropical teleconnections such as the El Niño–Southern Oscillation (Turner, 2004). In addition, the pronounced orography and land–sea contrast of the SOIs can induce localized variations in temperature, for example, via topographically induced föhn warming (King et al., 2017; Lu et al., 2023).

To date temperature variation and long-term trends in the SOIs have been estimated mainly based on meteorological records at Orcadas Station, Laurie Island, ~51 km from Signy Island (see Figure 1). Orcadas Station was established in 1903 by the Scottish National Antarctic Expedition and has then been operated by the Argentinian Antarctic Programme from 1904 to the present, providing the longest unbroken meteorological record south of 60°S (Zitto et al., 2016). The temperature record from Orcadas Station shows sustained warming during the 20th century, especially during summer, although the warming trend has levelled off in recent decades (Turner et al., 2019; Zitto et al., 2016). However, it remains uncertain whether the Orcadas record is representative of the SOIs. For instance, Jones (1995) examined annual temperature trends in the SOIs during 1961–1990 and found that these range from 0.58 to 0.87°C·decade^{-1}. Moreover, the trend at Orcadas Station over this period is around four times the trend of 0.19 ± 0.06°C·decade^{-1} reported by Turner et al. (2019) for the period 1903–2018. The substantial decadal-scale variability is possibly forced by changes in tropical teleconnections (Li et al., 2021).

Another research station, Signy Station, was established on Signy Island by the United Kingdom in 1944, which operated as a year-round meteorological station from 1947 to 1995. Signy and Orcadas Stations differ markedly in terms of their relative position to Coronation Island, the largest island in the archipelago that is 48 km

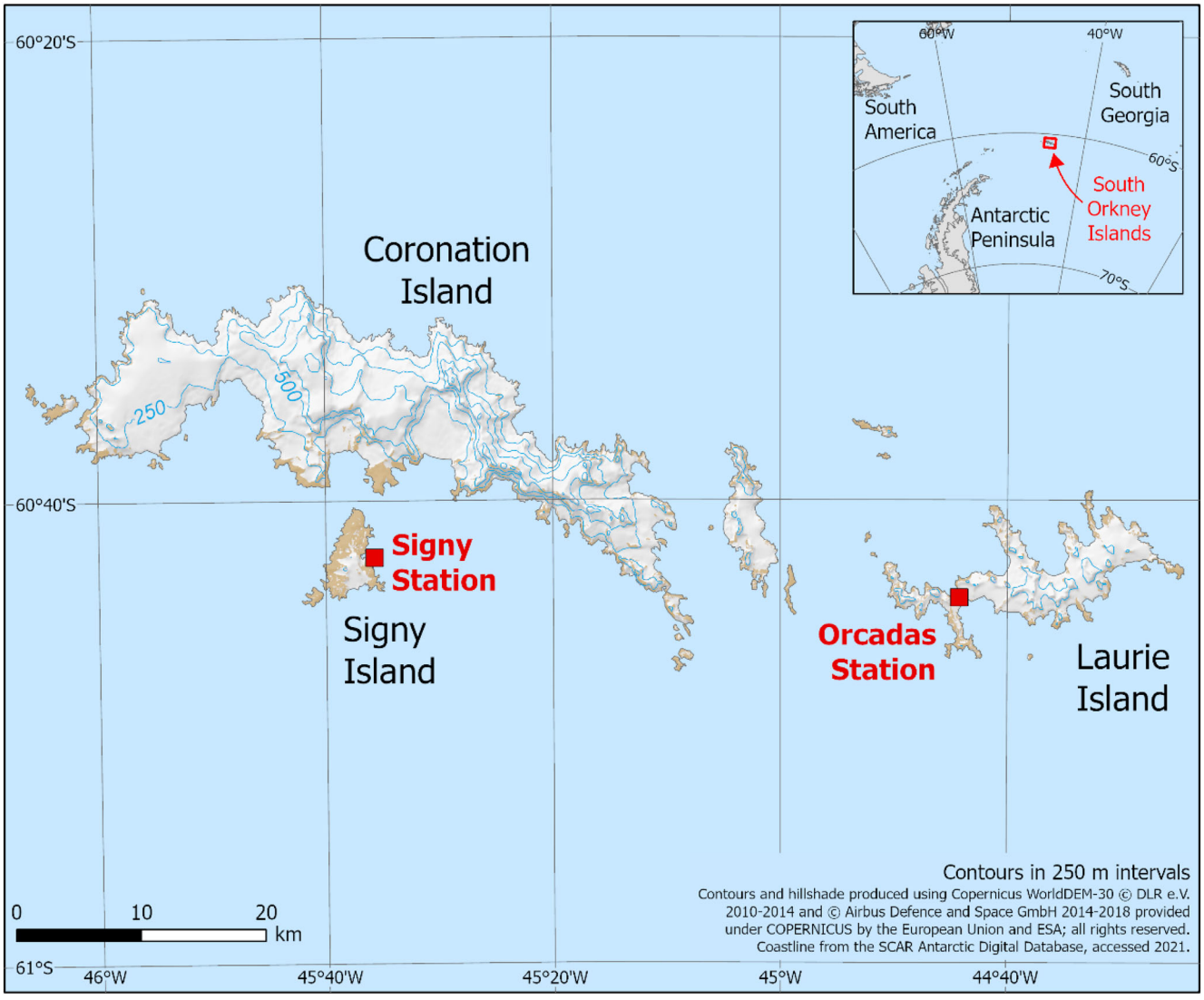

FIGURE 1 Topography of the SOIs and the locations of Signy and Orcadas research stations. The SOIs in the Southern Ocean is shown in the top right panel

long and with an east–west mountain spine reaching 1266 m a.s.l. Laurie Island is located to the east of Coronation Island while Signy Island is located to the south (Figure 1). This is critical because Coronation Island has a substantial orographic effect on the regional circulation (Chelton et al., 2004; King et al., 2017; Turner et al., 2021). Although the 45-year meteorological record from the station is useful for understanding spatiotemporal variability of temperature within the SOIs, this validation has not been carried out previously because synoptic records from Signy Station during 1947–1954 and 1970–1981 only existed in paper-based form and were archived at different repositories. Furthermore, Signy data outside these periods that were already digitized were not suitable for climate studies as they had not undergone proper quality control.

The lack of long-term temperature observations over the SOIs and the surrounding Southern Ocean has resulted in reanalysis data products being extensively used to study temperature variation and trends of the region (Bozkurt et al., 2020). Depending on the reanalysis products used, a widespread of climate trends has been reported in the Antarctic (Boisvert et al., 2020; Hobbs et al., 2020; Marshall, 2003; Swart & Fyfe, 2012). More importantly, the relatively coarse resolution of reanalysis products results in small, mountainous islands like the SOIs being misrepresented with local effects, for example, topographically induced föhn warming, being underrepresented (Alexander et al., 2009; Hosking et al., 2014; Jury, 2009; Yuan, 2004).

The valuable paper-based historical weather observations collected at Signy Station during 1947–1954 and 1970–1981 have recently been digitized by a team at the British Antarctic Survey. The team built an automated deep-learning Optical Character Recognition (OCR) model to extract the records from scanned versions of the paper copies automatically. The OCR model output was then put through a series of quality control procedures including human examination of the outputs. In this paper, we present the first study using the newly digitized, quality-controlled, historical observations from Signy Station to gain a better understanding of temperature variation and trends in the SOIs, and to better understand their spatial and temporal heterogeneity. Reanalysis representation of the seasonal cycle, variability and trends in regional temperature are also presented.

2 | DATA AND METHODS

2.1 | Station observations

Although meteorological observations at Orcadas Station are available as monthly averages since 1904 to present (Zazulie et al., 2010), subdaily records are only available from 1956 onwards and at standard synoptic hours (i.e., 0000, 0600, 1200, 1800 UTC). This dataset has undergone rigorous quality control as part of the SCAR READER project (Turner et al., 2004).

The recently digitized surface meteorological observations at Signy Station are accessable from the UK Polar Data Centre (Colwell and Lu 2023). Early observations at Signy Station were taken at the same standard synoptic hours during 1947–1949 and then every 3 h during 1950–1974. The records became twice daily (at 0000 and 1200 UTC) during 1975–1983 but mostly only one observation per day (at 1200 UTC) during 1976–1981. The collection interval returned to the standard synoptic hours during 1984–1987. Automated collection of data then started around late 1988, which allowed observations every hour to be collected during 1989–1995. Meteorological observations ceased when Signy Station became a summer-only operation after 1995. Unfortunately, the instruments at Signy Station were not regularly maintained in 1995, which resulted in spurious temperatures. Data from Signy Station during 1995 are thus excluded from this study.

In this study, a comparison of station temperatures is made for monthly and annual averages for the common period of 1947–1994. For the analyses that involve daily data, the comparison is made for 1956–1994. Hourly data at Signy and 6-hourly data at Orcadas are also used for a couple of case studies. To ensure consistency between estimates of daily temperature averages for each station, only the 0000 and 1200 UTC observations are used. During 1976–1981 the daily mean temperature at Signy Station was based only on data at 1200 UTC, as this was all that was available. However, the computation of daily means was found to be relatively insensitive to whether one (1200 UTC), two (0000 and 1200 UTC), or all four measurements at the standard synoptic hours were used, which is likely due to the relatively small diurnal cycle that characterizes the SOIs due to the strong maritime influence.

2.2 | Atmospheric reanalysis data sets

Near-surface temperatures from the global reanalysis product ERA5 (Hersbach et al., 2020) are compared with the station temperatures in terms of their synoptic variation and the seasonal cycle. The comparison is made based on data at the two synoptic hours chosen, that is, 0000 and 1200 UTC. ERA5 has a horizontal grid spacing of $0.25^\circ \times 0.25^\circ$ and 137 vertical levels. At this spatial resolution the SOIs are not well-resolved and the whole of the area of the island group is treated as ocean. The

ERA5 data are available from 1959 onwards. ERA5 fields are only well-constrained by satellite data from 1979 onwards hence, in common with all other reanalysis datasets, ERA5 is subject to large uncertainty/errors before 1979 (Marshall, 2003; Simmons & Hollingsworth, 2002). Examining the different pre- and post-satellite periods helps us to better evaluate the reanalysis biases and uncertainty. We thus separately examine the pre- and post-satellite periods whenever possible. In cases when the results do not differ, our results are based on the common period of ERA5 and station observations, that is, 1959–1994.

Monthly mean temperatures are also extracted from the JRA55, ERA20C and 20CR version 3 reanalysis products (Harada et al., 2016; Poli et al., 2016; Slivinski et al., 2019) for the purpose of comparing the long-term temperature trends. ERA20C and 20CR only assimilate surface and mean sea level pressure observations. Marine surface winds are also assimilated into ERA20C. Nearest neighbour interpolation is used to extract the corresponding values from the reanalysis data sets.

Note that only the observed pressure from Signy Station during 1955–1969 and 1982–1995 were assimilated by the reanalyses. The newly digitized temperatures from the station thus provide independent evaluations of all these reanalysis products.

2.3 | Sea surface temperature

To understand the long-term variation of the station-based temperatures, the monthly sea surface temperature (SST) data, version 4 from Hadley Centre for the period of 1947–2020, are used to estimate the SST trend over the extended region of the SOIs. The Hadley centre SST data were produced by combining the Marine Data Bank (mainly ship tracks) and International Comprehensive Ocean-Atmosphere Data Set up to 1981 and a blend of in situ and adjusted satellite-derived SSTs for 1982–onwards.

2.4 | Sea ice data

To study the influence of sea ice on air temperature variability and trends in the SOIs, we examine monthly average sea ice concentration (SIC) from Nimbus-7 SMMR and DMSP SSM/I-SSMIS passive microwave data, processed using the NASA Team algorithm (hereafter referred to as "NASA Team SIC") for the period of 1979–2020 during which Orcadas monthly mean temperatures are available.

Daily gridded Polar Pathfinder EASE-Grid Sea Ice Motion Version 4.1 data are also used to examine linkages between the station temperatures and sea ice drift. This dataset has been derived from a combination of buoy data, satellite data (including SMMR, SSM/I, SSMIS and AVHRR) and NCEP/NCAR reanalysis near-surface wind data. The data are gridded onto a Lambert-Azimuthal Equal Area Grid with 25 km grid resolution and encompass the period from November 1978 to the present day.

2.5 | Trends and statistical tests

Temperature trends are estimated from all available monthly data for the two stations and the reanalysis data sets. The nonparametric Mann–Kendall test is used to test the significance of the temperature trends (Alexander & Arblaster, 2009). The test has been widely used for evaluating the presence of monotonic trends in datasets that do not obey a Gaussian distribution, as it makes no assumption of normality.

3 | RESULTS

3.1 | Temperature distribution, climatology and seasonal cycle

3.1.1 | Station observations

Figure 2a shows the normalized histogram of the 12-hourly temperatures at Signy and Orcadas for all months during 1956–1994. Both histograms are negatively skewed. This is a consequence of the negatively skewed distribution of winter (June–September) temperatures (Figure 2c) as the temperatures in summer follow a near-normal distribution, with a single sharp peak just above freezing point reflecting the dominant role of the cold Southern Ocean temperatures (Figure 2b). The temperature histograms agree well between Signy and Orcadas except that Signy ones have a smaller kurtosis (i.e., the sharpness of the peak) and a warmer tail, with the effect most pronounced in summer. Thus, there is a stronger warm influence by extreme high temperature events at Signy than Orcadas.

The annual mean air temperatures at Signy and Orcadas stations are −3.4 and −3.6°C, respectively (Table 1). In summer, the mean temperature of the islands is around 0.5°C with Signy being 0.4°C warmer than Orcadas. In winter, the average temperature of the islands is around −8°C with Signy temperature being slightly colder than Orcadas. In terms of the diurnal cycle, the temperatures at both stations peak around 1800 UTC (∼1500 LST) and trough at 0600 UTC (∼0300 LST) with a small amplitude, that is, 0.7°C in winter and 1.2°C in summer.

The surface winds are stronger at Signy than Orcadas as Coronation Island acts as a barrier to the westerlies

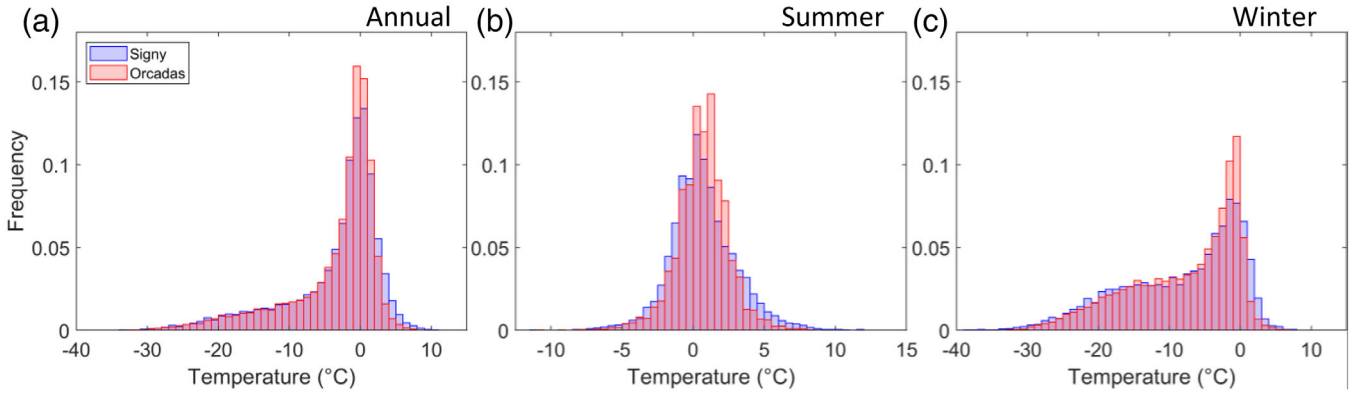

FIGURE 2 (a) Normalized histograms of 12-hourly 2 m temperature observed at Signy (blue) and Orcadas (red) for the common period 1956–1994. (b) Same as (a) except for the extended summer (December–March). (c) Same as (a) except for extended winter (June–September)

TABLE 1 Annual, summer and winter temperature (°C) mean, range, trend and the amplitude of diurnal cycle (ADC) (0600–1800 UTC) at Signy and Orcadas for their common period of 1956–1994

	Annual				Summer (December–March)				Winter (June–September)			
Station	**Mean**	**Range**	**Trend**	**ADC**	**Mean**	**Range**	**Trend**	**ADC**	**Mean**	**Range**	**Trend**	**ADC**
Signy	−3.4 ± 6.9	−40 to 20	*0.20*	0.9	0.8 ± 2.3	−13 to 20	**0.24**	1.3	−8.3 ± 8.2	−40 to 11	0.07	0.7
Orcadas	−3.6 ± 6.3	−39 to 14	*0.17*	0.8	0.4 ± 1.8	−12 to 14	**0.20**	1.0	−7.9 ± 7.6	−39 to 8	0.05	0.7

Note: Trends that are statistically significant at $p = 0.05$ (0.1) are highlighted as bold (italic).

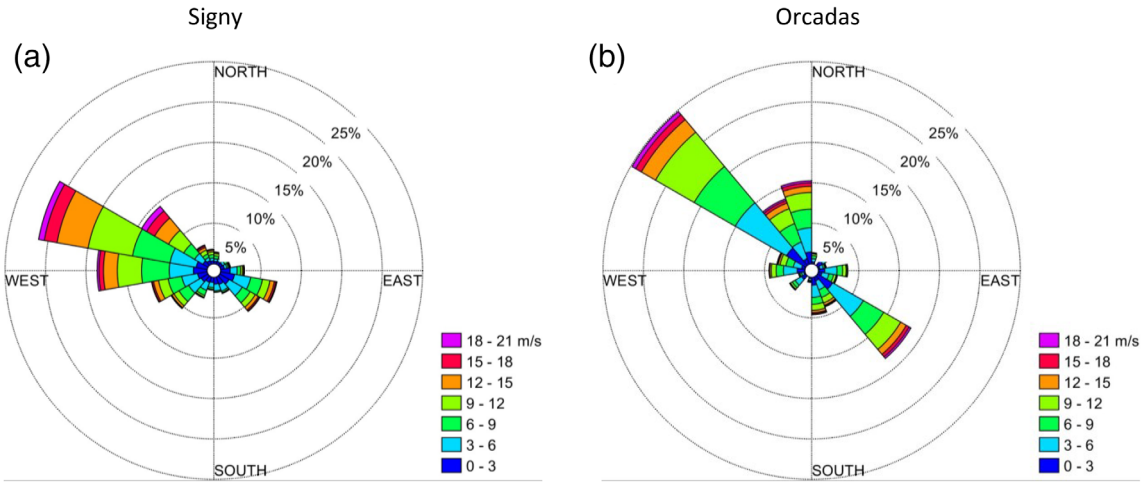

FIGURE 3 The 10-m wind rose for Signy (a) and Orcadas (b) constructed from synoptic observations during 1956–1994

(Figure 3). The year-around average wind speed is 7 $m \cdot s^{-1}$ at Signy but 6 $m \cdot s^{-1}$ at Orcadas. The winds are strongest in winter with 10 $m \cdot s^{-1}$ on average at Signy and ~8 $m \cdot s^{-1}$ at Orcadas. The wind directions at both stations are bimodal (Figure 3). At Signy, the dominant wind direction spans 220°–320°, signifying the prevailing westerlies. There is a second peak at 100°–140°. At Orcadas, the dominant direction is northerly and northwesterly, that is, 300°–360°. There is also a second peak at 120°–140°. The bimodality at Orcadas reflects the barrier effects of Coronation Island against the prevailing westerlies and the southeasterly winds.

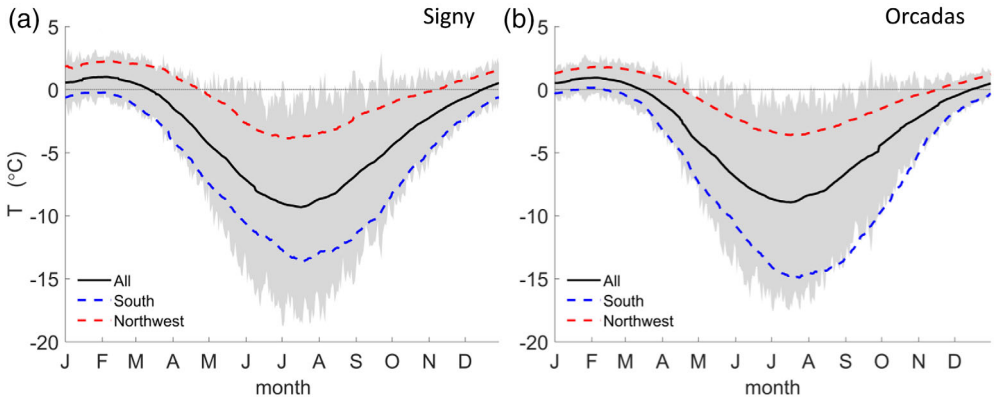

FIGURE 4 (a) Annual cycle of the observed temperature at Signy during 1956–1994. The black, red dashed and blue dashed lines are the 91-day running averages of all wind sectors, when the winds are northwesterly (280°–360°) and southerly (120°–260°), respectively. The grey shaded region indicates the one standard deviation of daily averages. (b) Same as (a) but for Orcadas

TABLE 2 Annual, summer and winter temperature mean at Signy and Orcadas for the wind sectors of northwesterly (280°–360°) and southerly (120°–260°) during 1956–1994

	Annual		Summer (December–March)		Winter (June–September)	
Station	**Northwest**	**South**	**Northwest**	**South**	**Northwest**	**South**
Signy	−1.2 ± 5.3	−5.6 ± 7.0	1.4 ± 2.3	−0.4 ± 2.2	−4.2 ± 6.6	−11.8 ± 7.5
Orcadas	−1.2 ± 4.2	−6.4 ± 7.4	1.3 ± 1.6	−0.3 ± 1.7	−4.0 ± 5.3	−13.2 ± 7.2

Figure 4a shows the seasonal cycle of temperatures at Signy together with the one standard deviation of daily mean temperature. In summer, the temperatures at the station vary around the freezing point with a standard deviation of daily temperature of $\sigma = 2.3°C$ (Table 2). The temperature variation is evidently larger during winter ($\sigma = 7.9°C$); the station temperatures frequently switch from above freezing point to below −30°C in a matter of days. The large variation in winter temperature is dictated by the presence or absence of sea ice and by cyclonic activity that can advect warm airmasses from the open oceans or cold air from the sea-ice covered Weddell Sea (Turner et al., 2021; Wille et al., 2019).

Figure 4a demonstrates that the 91-day averaged cycle of temperatures for the days with winds from the northwesterly sector (280°–360°) closely tracks the upper bound of the one standard deviation of the daily temperature while that associated with the southerly sector (120°–260°) track the low bound, especially in summer. The prevailing westerlies can bring in either cold or warm air masses to Signy depending on the conditions upstream, for example, sea ice or open ocean in the region between the Antarctic Peninsula and the SOIs (not shown). The temperature averages for this dominant wind sector at Signy Station thus closely track the all-sector mean. Extreme cold events occur in winter and when the winds are southerly. In contrast, extreme high-temperature events occur predominantly in summer and when the winds are northwesterly (Lu et al., 2023). A similar seasonal cycle of temperatures is found at Orcadas though the day-to-day temperature variability is smaller (Figure 4b).

3.1.2 | ERA5 representation

The temperatures extracted from ERA5 at the station locations are highly correlated with observations at both Orcadas and Signy (Table 3). For annual averages, the correlation coefficient reaches as high as 0.96 in the post-satellite period (1979–1994) but reduces to around 0.80 for the pre-satellite period (1956–1978). Summer correlations are substantially lower, with the r values ranging between 0.6 and 0.71 (Table 3). Intriguingly, the summer correlations do not show much improvement during the post-1979 period, when the quality of ERA5 is known to have been improved. The underrepresentation of summer temperatures by ERA5 may be explained by the fact that the entire SOIs are defined as ocean. High-temperature events over the SOIs would be more likely to be underestimated by ERA5 because oceans warm more slowly than

land. Such biases are stronger in summer because the SOIs are surrounded by open ocean in summer but sea ice in winter.

Figure 5 shows box plots of the daily temperature at Signy and Orcadas from station observations and those extracted from ERA5; both are grouped according to the

TABLE 3 Correlation of station synoptic observations with ERA5, all measurements included

	Annual		Summer (December–March)		Winter (June–September)	
Station	**1959–1978**	**1979–**	**1959–1978**	**1979–**	**1959–1978**	**1979–**
Signy	0.79	0.95	0.60	0.69	0.76	0.94
Orcadas	0.84	0.96	0.62	0.71	0.77	0.95

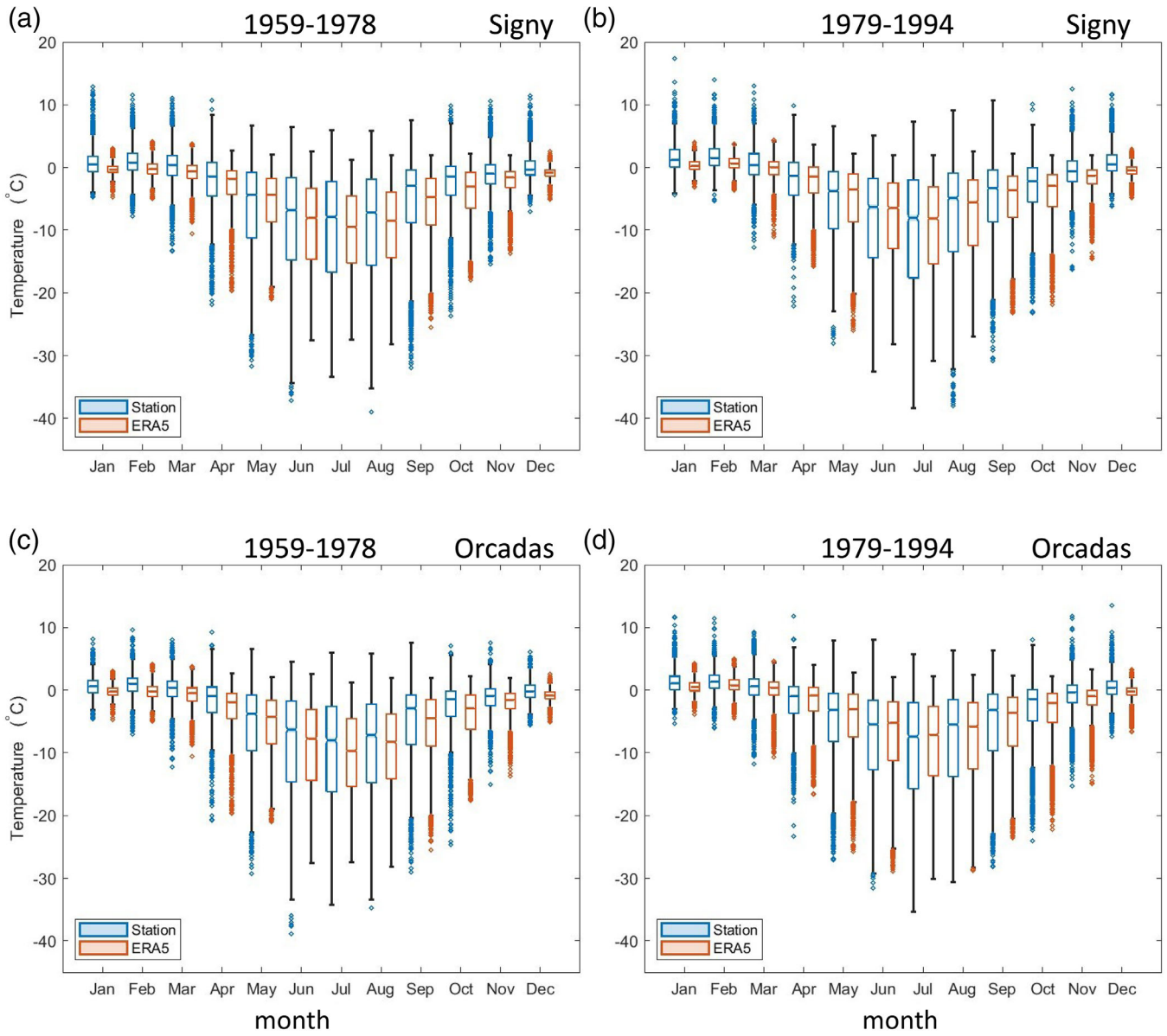

FIGURE 5 Box plots of the observed (blue) and ERA5 (red) daily temperature for each calendar month at Signy Station (a, b) and Orcadas (c, d) and during 1959–1978 (a, c) and 1979–1994 (b, d). The median temperature for a given month is shown as the line inside the box while the lower and upper quartiles are shown as the bottom and top edges of the box. The whiskers extend below and above the box represent 1.5 times the inter-quartile range (IQR) of the daily temperatures while the small circles that extend from the whiskers correspond to the outliers, which is defined as a value that is more than 1.5 times the IQR away from the bottom or top of the box

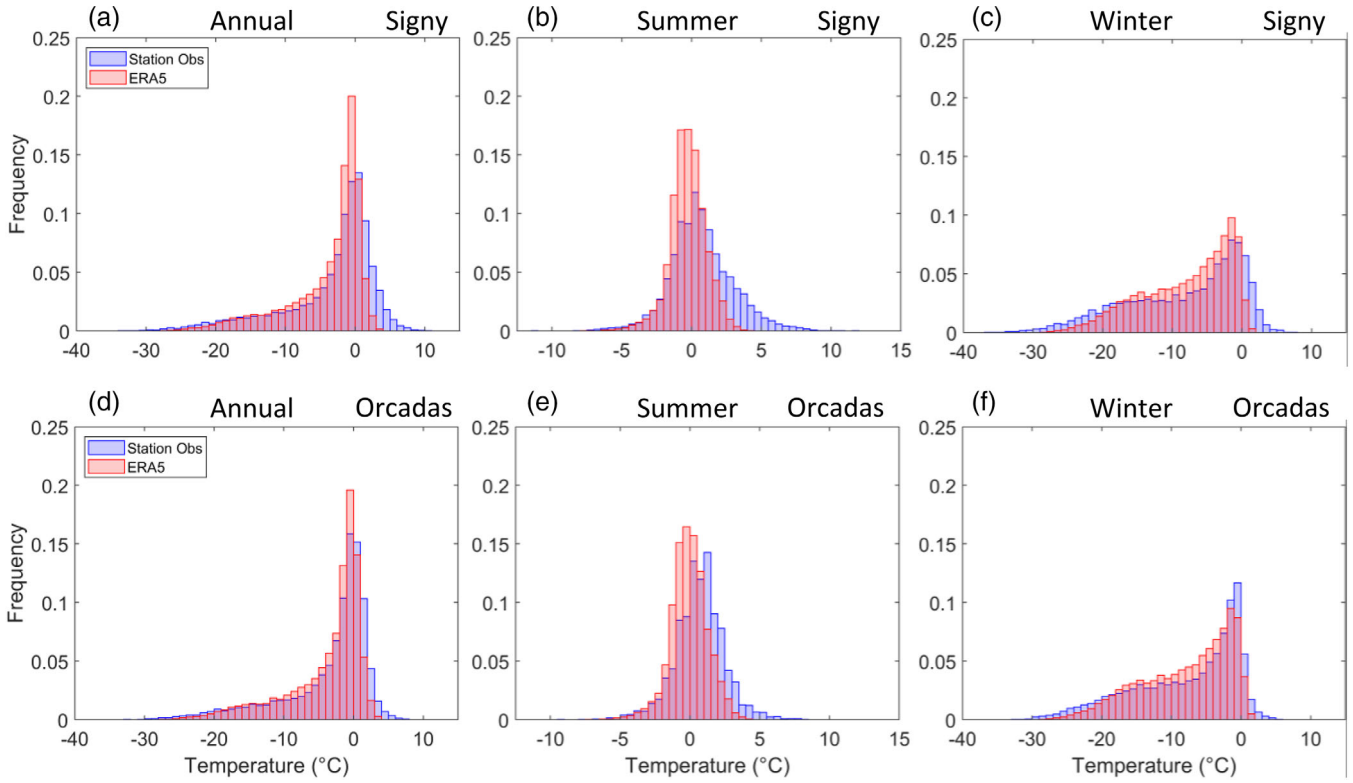

FIGURE 6 (a) Normalized histograms of 12-hourly temperature observations at Signy (blue) and corresponding temperature extracted from ERA5 at the same location (red) for the period 1959–1994. (b, c) Same as (a) except for the extended summer (December–March) and winter (June–September). (d–f) Same as (a–c) except for Orcadas

calendar months for the post- and pre-satellite periods. At Signy Station, ERA5 generally captures the seasonal cycle of station temperature well, especially during the post-satellite period (Figure 5b). It is, however, evident that ERA5 significantly underestimates the observed Signy temperature in summer by 0.9°C on average ($p \leq 0.05$). During the pre-satellite period, ERA5 also underestimates the median temperatures in winter, for example, by as much as 2.7°C in July (Figure 5a). Very similar results are obtained for Orcadas Station though the magnitude of underestimation becomes smaller (Figure 5c,d).

Figure 6 compares the normalized histograms of 12-hourly temperature at the stations with that derived from ERA5 for the period 1959–1994. It is evident that ERA5 underestimates both the warm and cold tails of the histograms. Underestimation is more pronounced for the warm tail than the cold tail, resulting in an overall cold bias in ERA5. In addition, underestimation is most pronounced for Signy as the reanalysis does not capture the magnitude of the extreme high temperature events, defined as those exceeding the 95th percentile of the temperature distribution (Figure 6b). Also see Lu et al. (2023).

Figure 7 provides two examples of how hourly ERA5 data compare with station observations during January 1994 and August 1994, when which Signy was recording hourly data. ERA5 has a persistent cold bias in January 1994. The largest cold bias occurs at 1600 UTC 19 January 1994, when temperatures at Signy reached 11.4°C while Orcadas had a temperature of only 1.7°C (this is the average value between 1200 and 1800 UTC on 19 January 1994). At the same time, ERA5 has a temperature of 2.8°C at both stations. In August 1994, ERA5 tends to underestimate temperature variability (i.e., ERA5 has a cold bias during warm periods and a warm bias during cold periods) though the relative magnitude of the biases is smaller than for the summer example.

3.2 | Trends and multidecadal variation

The annual mean temperature at both stations only shows a weak, though statistically significant, positive trend for the period of 1947–1994 period (Table 1). For Signy it is 0.20 ± 0.22°C·decade^{-1} ($p \leq 0.10$) (also see Figure 8a). However, the summer mean temperature shows a more significant positive trend at Signy (0.24 ± 0.09°C·decade^{-1}, $p \leq 0.01$; Figure 8b), with an equivalent trend at Orcadas of 0.20 ± 0.14°C·decade^{-1} ($p \leq 0.05$). The reason why the annual mean temperature

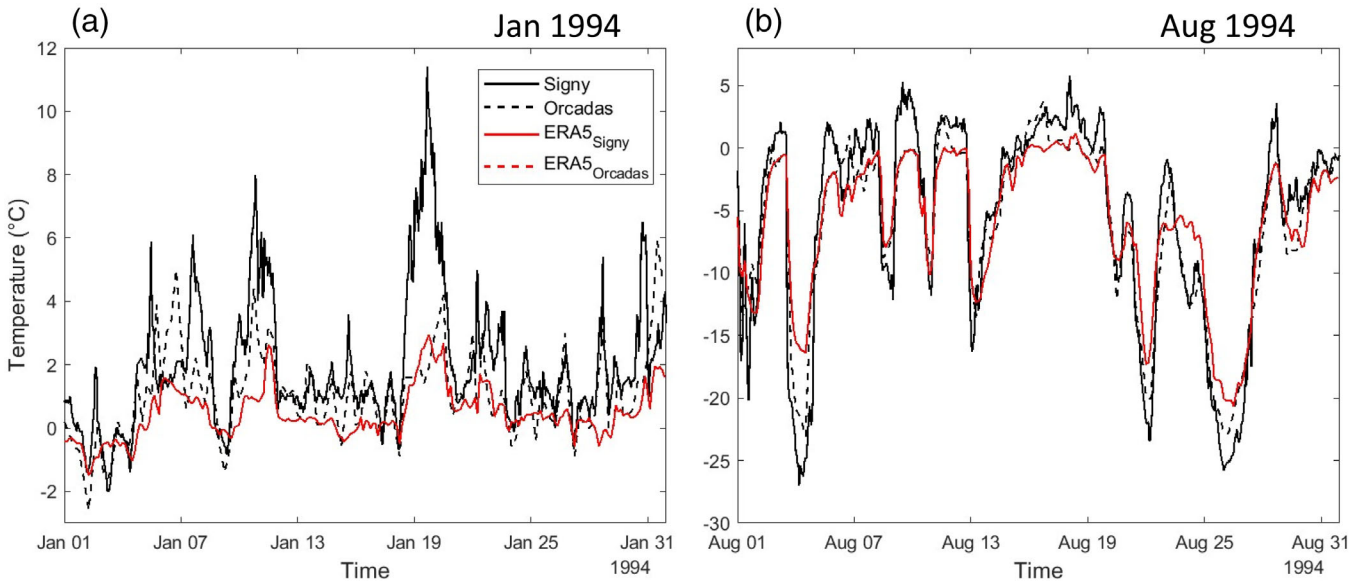

FIGURE 7 Time series of observed synoptic temperatures at Signy (black solid) and Orcadas (black dashed) comparing with those extracted from ERA5 at the same location of the stations (red solid and dashed) for January 1994 (a) and August 1994 (b). Note that both Signy records and ERA5 temperature are hourly while the records from Orcadas are 6-hourly. Also, ERA5 temperatures at Orcadas is identical to those at Signy

at the stations only has a weak positive trend is because September–October mean temperatures decrease with time (Figure 8c).

The seasonal cycle of temperature at Signy is not stationary during 1947–1994 (Figure 9a). The seasonal-cycle amplitude is significantly larger during 1972–1994 than during 1947–1970. The larger seasonal cycle amplitude during 1972–1994 is due to higher summer temperatures but lower temperatures in early winter (June) and spring (September–October). Lower temperatures in spring during 1972–1994 are also evident at Orcadas (Figure 9b).

3.3 | Connection with regional circulation variability

To put these observed trends and the multidecadal variation of station temperature into the context of regional variation, Figure 10a shows the ERA5 summer mean 2 m temperature difference between the periods of 1972–1994 and 1959–1971, that is, mean of December–March mean, December 1972–March 1994 minus mean of December–March mean, December 1959–March 1971.

The summer temperatures in the SOIs are significantly warmer (by up to 1°C, $p \leq 0.01$) during 1972–1994 than the earlier period, which agrees with observations (see Figure 8b). The largest temperature differences are found near the tip of the Antarctic Peninsula where the increase of temperature is over 2°C. These summer temperature increases during 1972–1994 are associated with a deepened Amundsen Sea Low as well as low pressure anomalies over the west of D'Urville Sea, Western Pacific Ocean (90°–130°E, 55°–65°S) while high-pressure anomalies are found north of the SOIs at 60°–30°W, 40°–55°S and over the East Antarctica–Southern Ocean sector. These mean sea level pressure (MSLP) anomalies are accompanied by enhanced northwesterlies on the west side of the Drake Passage and enhanced northerlies at 40°–60°W, 50°–75°S on the east side (Figure 10b,c). Such circulation anomalies would bring in warm air from both the Pacific and South Atlantic Ocean to the SOIs (Figure 10d), consistent with the higher summer temperature recorded at the stations during 1972–1994.

Winter temperatures near the SOIs are ~0.6°C colder during 1972–1994 than 1959–1970 though the differences are not statistically significant (Figure 11a). The regional temperature differences are, however, dominated by anomalous warmth near the Antarctic Peninsula, along the Antarctic coast, over the southern part of the Weddell Sea, southern Pacific and southern Atlantic. These regional temperature differences are associated with the anomalous high-pressure anomalies over the Amundsen-Bellingshausen Sea and low-pressure anomalies over the Weddell Sea (Figure 11b). These pressure anomalies induce enhanced southerly winds near the Drake Passage and an anomalous cyclonic circulation over the Weddell Sea (Figure 11c). As part of this cyclonic circulation, the southerly winds on the eastern side of the Antarctic Peninsula advect sea ice from the interior of the Weddell Sea

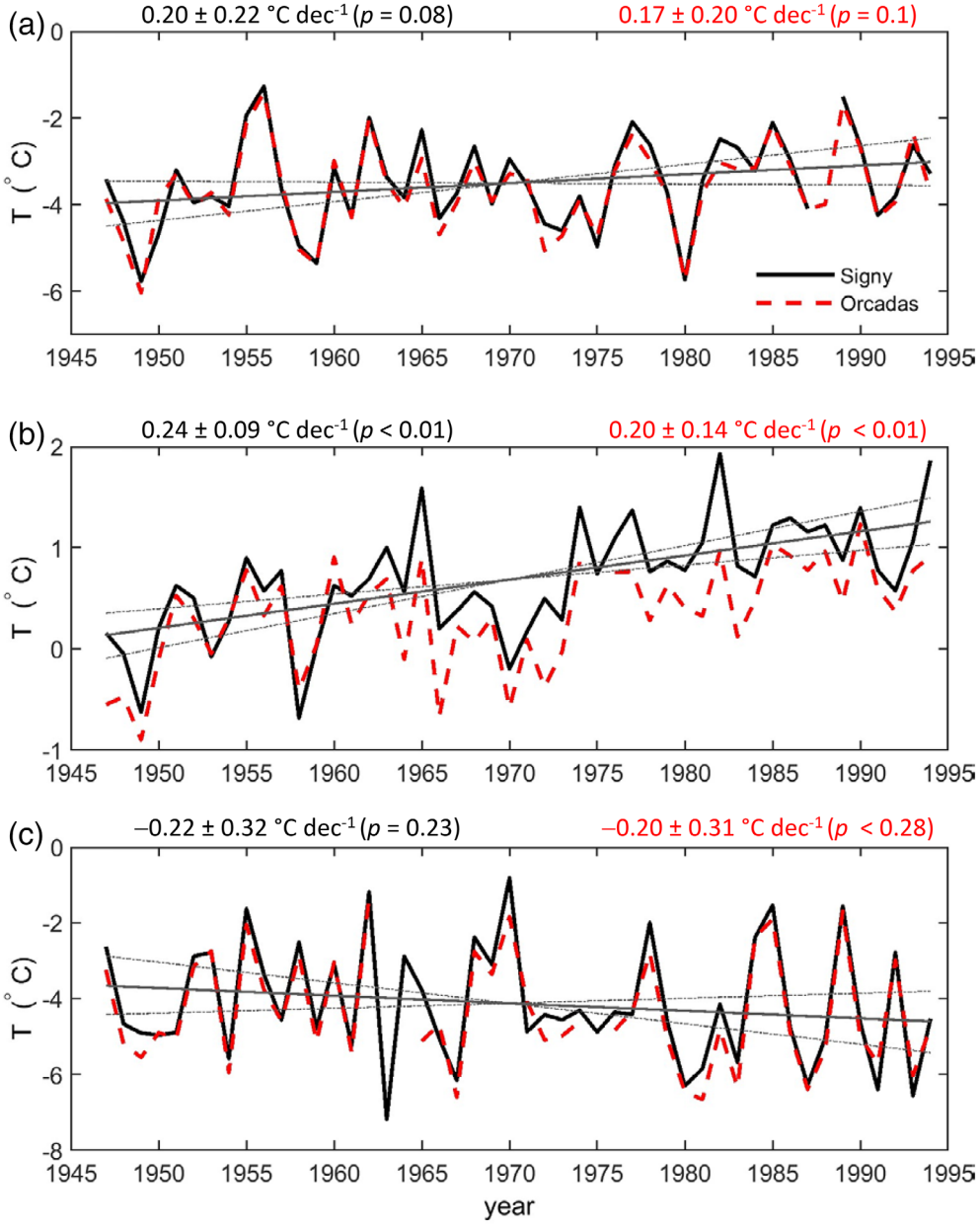

FIGURE 8 (a) Annual mean temperatures (°C) for Signy (black) and Orcadas (red dashed) for the period of 1947–1994. The corresponding trends and 95% confidence intervals are provided at the top of the panel. The trend and confidence interval of Signy are also shown as the thin black and dotted lines. (b, c) Same as (a) except for summer (December–March) and September–October

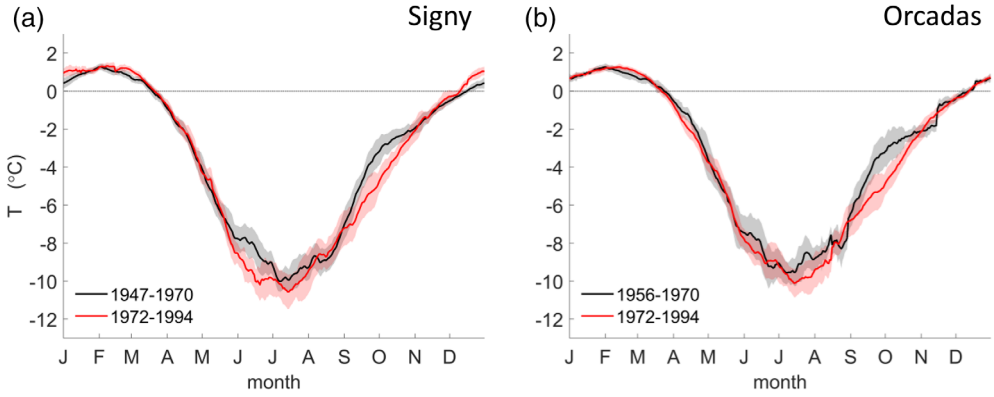

FIGURE 9 (a) Seasonal cycle of the observed temperature for 1947–1970 (black) versus 1972–1994 (red) at Signy with the grey- and red-shaded regions indicating the 95% confidence of the 31-day centred running averages. (b) Same as (a) but at Orcadas for 1956–1970 (black) and 1972–1994 (red)

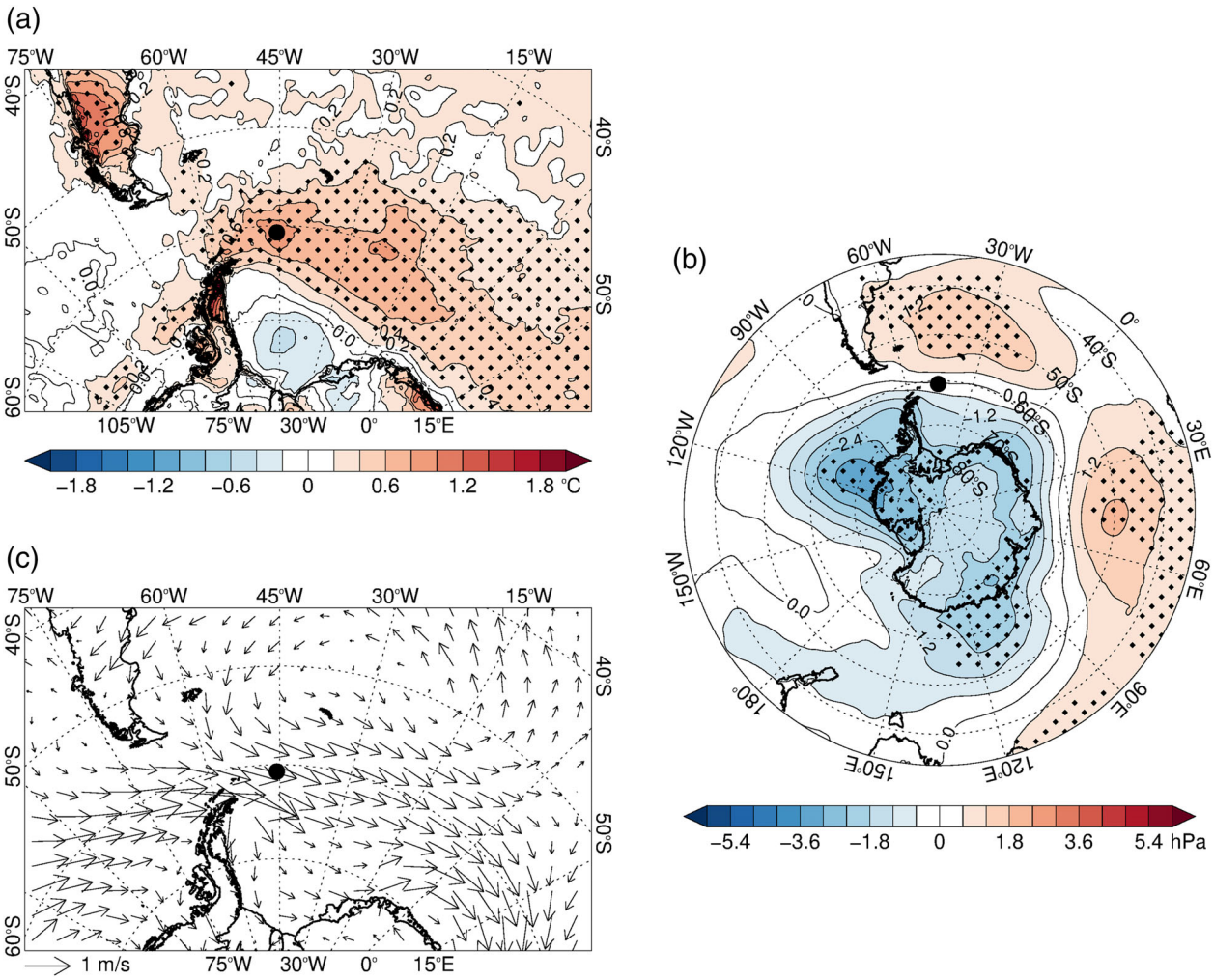

FIGURE 10 (a) Composite differences of 2 m temperature in summer (December–March) between 1972–1994 and 1959–1971 periods for the extended region of the SOIs. Stippled regions indicate the differences are statistically significant at $p = 0.05$ level. (b) Same as (a) except for MSLP over the extratropical Southern Hemisphere. (c) Same as (a) except for 10 m wind fields

towards the SOIs, thus leading to the colder winter temperature there during 1972–1994.

Figure 12a shows the linear trend of summer SSTs over the extended region of the SOIs and for the period of 1947–2020. The most significant trends of the summer-mean SSTs over the extended region of the SOIs are detected over the Brazil Falkland Confluence (BFC), that is, 45°–58°W, 35°–50°S, which is located directly north of the SOIs, indicated by the yellow box in Figure 12a. The summer SST trend for this region reaches 0.18°C·decade^{-1} over the period, which is statistically significant ($p << 0.01$) (Figure 12b). A significant trend is also obtained for the post-satellite era, that is, 1979–2020 (0.11°C·decade^{-1}, $p = 0.03$). These results agree with previous studies that the SST isotherms of the Brazil Current exhibit a significant southward expansion since 1854 with a significant warm trend over the BFC zone (de Souza et al., 2019; Zavialov et al., 1999).

The BFC is where the warm and salty Brazil Current from the tropics is met by the colder and fresher water of the Falkland Current from subpolar origins (Gordon, 1989). The BFC has the SST ranging from 7 to 18°C on average and is marked by a complex array of strongly contrasting water types. The BFC is also a region with complex dynamical processes and intense cyclogenesis (Hoskins & Hodges, 2005). We nevertheless find that the summer mean SSTs averaged over the BFC zone are significantly correlated with the summer averaged temperature observed at Signy ($r = 0.39$, $p = 0.008$) for the period 1947–1994 and at Orcadas ($r = 0.43$, $p = 5.7\text{e-}4$) for the period 1947–2020. With the enhanced northerly winds (Figure 10c), the warm trend of the SST over the BFC zone would provide favourable conditions for föhn events in summer at Signy as northerly winds flow over Coronation Island (King et al., 2017; Lu et al., 2023), which may explain the larger summer temperature trend at Signy (Figure 8b).

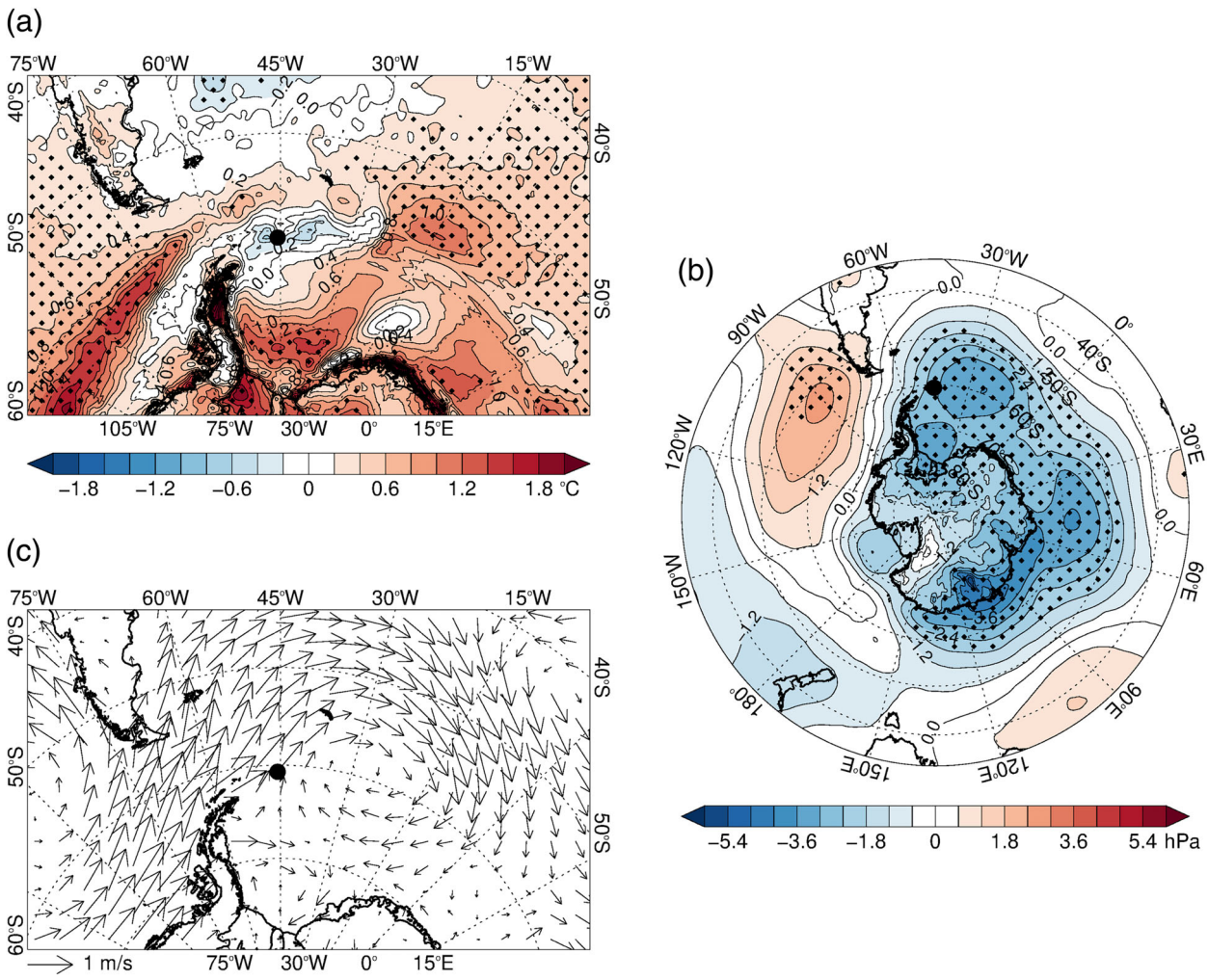

FIGURE 11 Same as Figure 10 except for winter (June–September)

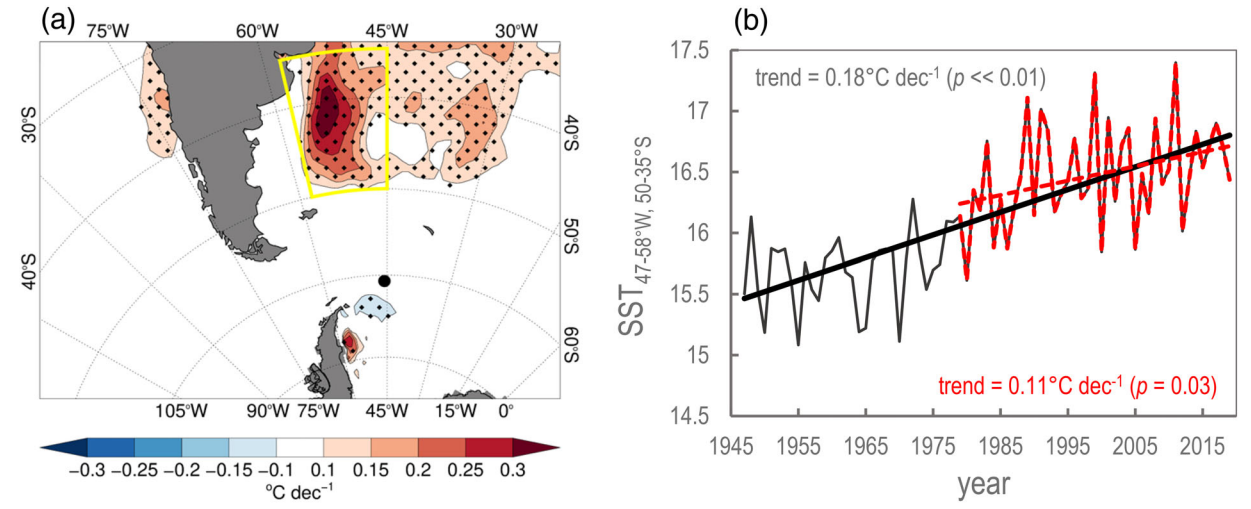

FIGURE 12 (a) Linear trend of the SST (°C·decade^{-1}) during summer (December–March) during 1947–2020 with the SOIs shown as the black dot. Stippled regions indicate that the trends are statistically significant at $p \leq 0.05$ and the absolute value of the trends are greater than 0.1°C decade^{-1}. (b) Time series of the summer SST averaged over the BFC, that is, the yellow box (i.e., 35°–50°S, 45°–58°W) in (a) with the linear trends for the entire period (1947–2020) and the satellite era (1979–2020) shown as the black solid and red dashed lines

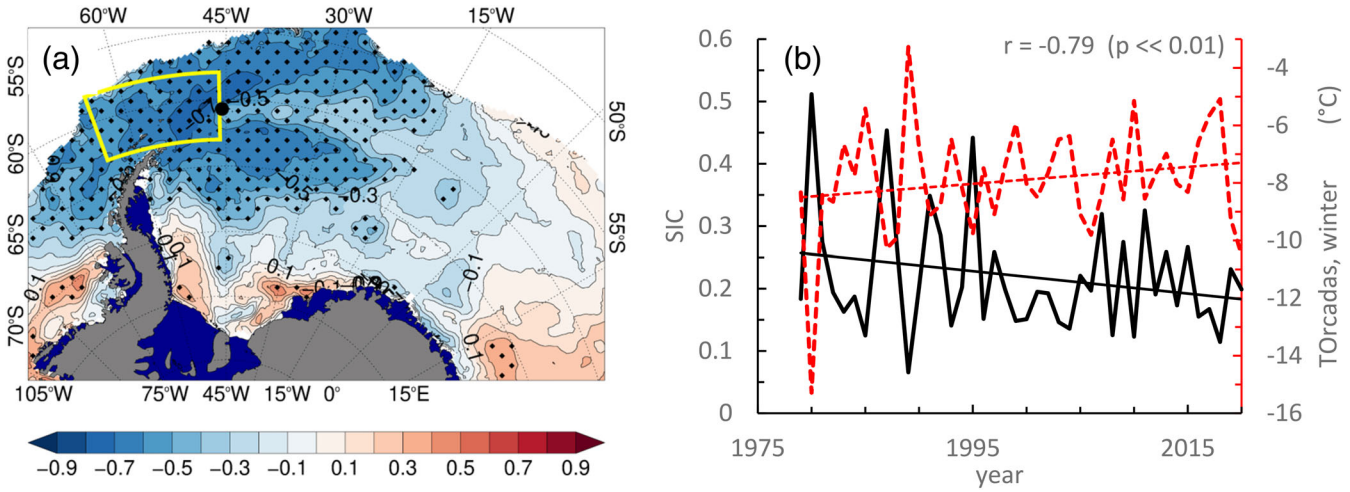

FIGURE 13 (a) Correlation between June–September temperature at Orcadas and the SIC of NASA Team v2.0 over the extended Weddell Sea sector for the period of 1979–2020. To remove noise, regions where the mean Jun–Sep SIC is less than 0.1% are masked out. (b) Time series of June–September averaged SIC (black solid) at 46°–65°W, 58°–63°S, indicated by the yellow box in (a), and June–September averaged station temperature at Orcadas (red dashed)

3.4 | The role of sea ice

To better understand the connection between the station temperature and sea ice, Figure 13a shows the correlation between winter temperature (June–September) at Orcadas and NASA Team SIC for the period of 1979–2020. Orcadas temperature is used here because the records extend to present day and thus have the longest overlapping periods with the SIC data. Because the winter temperatures at Orcadas and Signy are very similar, the results reported in the section should be representative of both stations.

It is evident that the station temperature anomalies during winter are negatively correlated with the SIC over the Bellingshausen Sea and north of the Weddell Sea. The highest correlation magnitude is found at 46°–65°W, 58°–63°W ($r = 0.79$), upstream of the SOIs. The negative correlation between the June–September averaged Orcadas temperature and the June–September averaged SIC over 46°–65°W, 58°–63°S for the period of 1979–2020 is evident in Figure 13b. Significant positive correlations are also found over the coastal polynyas in the southwestern Weddell Sea. Thus, when the wind within the Weddell Sea is anomalously southerly, the circulation is conducive to transport of sea ice away from the Ronne Ice Shelf. Concurrently, cold temperatures are more likely to be recorded in the SOIs.

To appreciate how SOIs temperature relates to regional sea ice on shorter timescales, we examine the correlation between Orcadas daily temperature and sea ice drift speed during June–September over the Weddell Sea region. With the sea ice field leading Orcadas temperature by 1 day, it is evident that Orcadas winter temperature is positively correlated with the zonal velocity of sea ice near the SOIs and in the northeast of the Weddell Sea but negatively correlated in the southwest of the Weddell Sea. The station temperature is however negatively correlated with the meridional component of sea ice drift velocity within the Weddell Sea (Figure 14b). These correlation patterns are very similar to the correlations between the Orcadas temperature and 10 m winds (Figure 14c,d). These results suggest that the connection between the sea ice and Orcadas temperature is primarily wind driven. Orcadas temperature increases as sea ice is advected away from the SOIs by either enhanced westerlies or northerlies. Conversely, the southerly winds advect sea ice from the Weddell Sea towards the SOIs, which cools the temperature in the SOIs. The meridional wind anomalies have a compounding influence on the SOI temperature, which not only bring in warm (cold) air from the South Atlantic Ocean (the Weddell Sea) but also advect sea ice away (towards) the SOIs. For instance, the southerlies were enhanced during 1972–1994 (Figure 11d); thus, colder winter temperatures were recorded in the SOIs during those years (Figure 9).

3.5 | Uncertainties in reanalyses in representing long-term trends

Here we examine the ability of reanalyses that extend back in time beyond 1979 to reproduce station observed temperature trends at Signy and Orcadas. Figure 15a

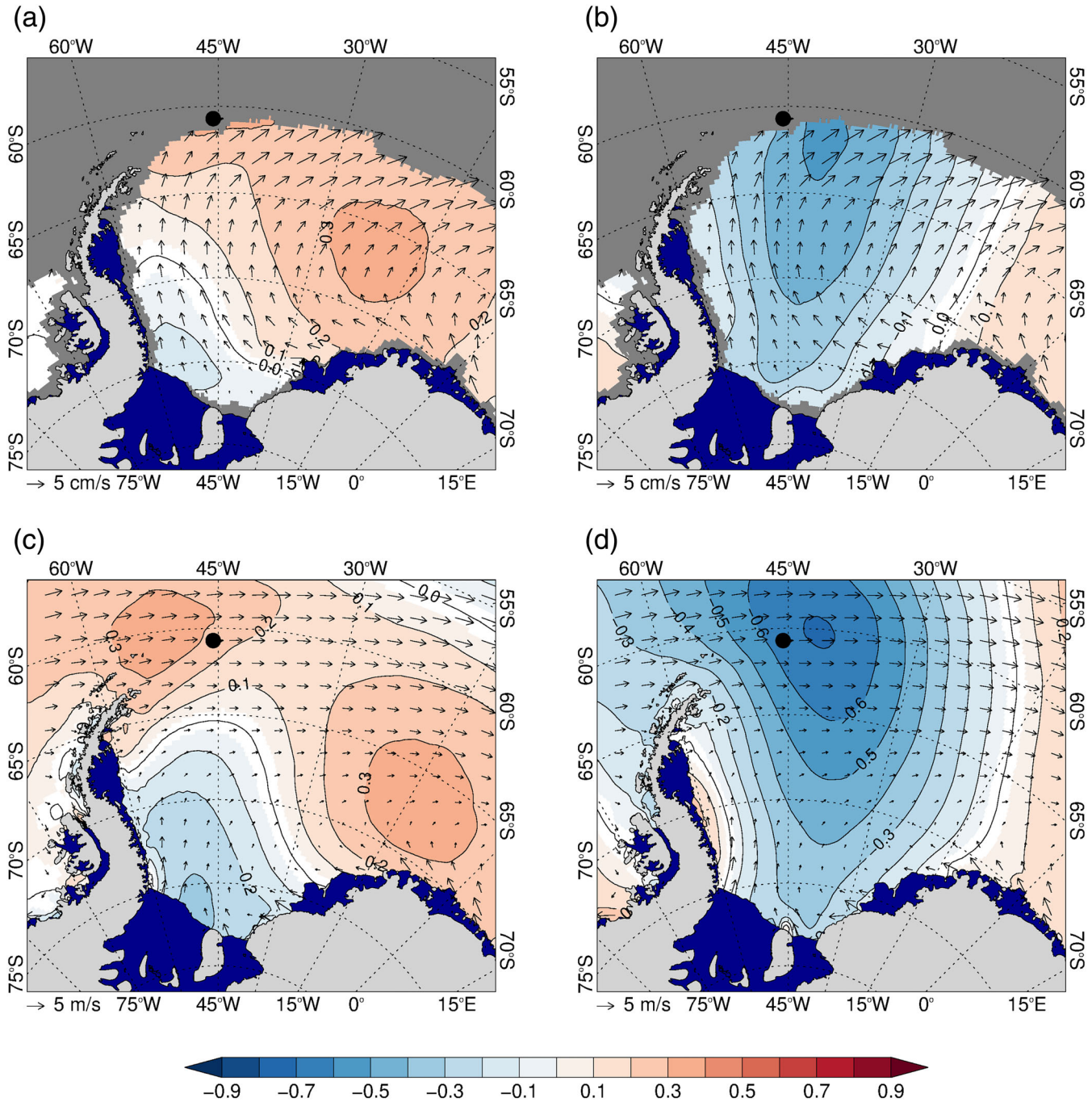

FIGURE 14 (a) Correlation (colour) between daily temperatures at Orcadas during winter (June–September) and the zonal component of Polar Pathfinder daily sea ice drift velocity (in $cm \cdot s^{-1}$) over the Weddell Sea sector with the sea ice drift velocity field leading the Orcadas temperature by 1 day. The climatological winter sea ice drift speed is overlayed as the vectors. The coloured contours are masked in white where the correlations are not significant at $p = 0.05$. Ice shelves are shown as dark blue. The dark grey region indicates where daily sea ice motion data were not available for more than 10% of the days. (b) Same as (a) except for the meridional component of sea ice drift velocity. (c, d) Same as (a, b) except that the sea ice drift fields are replaced by ERA5 10 m winds with no time lag between the station-temperature and ERA5 winds. Similar results are obtainable using Signy data (not shown)

compares the annual mean temperature at Signy with those from reanalysis data sets for the period of 1947–1994. All the reanalyses capture the interannual variation of station temperature exceedingly well after 1975 with ERA5 closest to the station observations, which is consistent with previous evaluation (Zhu et al., 2021). However, a cold bias can clearly be seen in most of the reanalyses before 1975. The cold bias

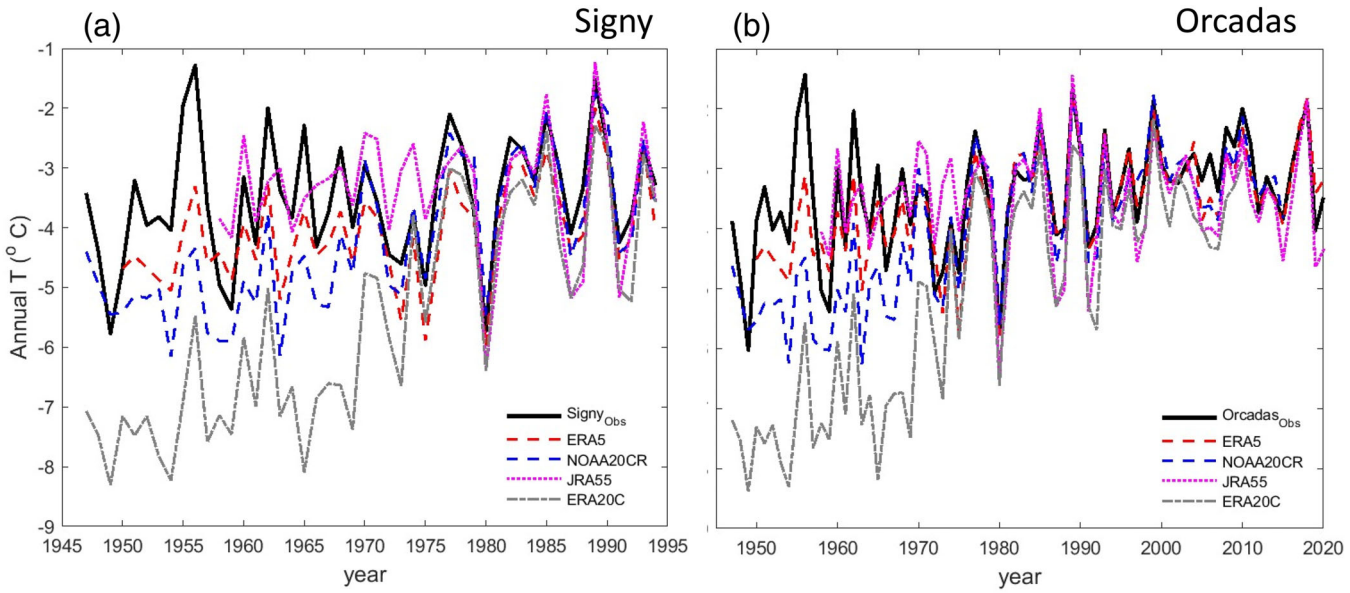

FIGURE 15 (a) Station-based annual mean temperatures (°C) of Signy (black) compared with four different reanalysis products, that is, ERA5, 20CR, JRA55 and ERA20C for 1947–1994. (b) Same as (a) except for Orcadas and for the period of 1947–2020

remains even after 1979 though the magnitude is noticeably smaller. The largest bias is associated with ERA20C, which greatly underestimates the station temperatures by more than 3°C before 1975. The early period underestimation of temperature is primarily associated with summer months (cf., Figures 5 and 6 as an example), which results in spuriously large positive temperature trends in ERA20C, 20CR and ERA5. On the contrary, JRA55 tends to overestimate the station temperatures. Thus, no significant temperature trend is detected in JRA55, which appears to be consistent with the inability of this reanalysis to reproduce the regional change in SAM structure prior to 1979 (Marshall et al., 2022). The large spread among the reanalyses makes reanalysis temperature trends highly uncertain before 1979.

Similar spread and biases can be seen in Orcadas where data are extended forward to 2020 (Figure 15b). In comparison with the observations, cold biases of up to ~1°C are evident in some years after 1979. Thus, the cold bias is not limited to the pre-satellite period. ERA5 agrees with Orcadas temperature slightly better than other reanalysis datasets with a maximum cold bias of 0.7°C, consistent with Figure 5.

The biases are particularly larger in winter than in summer for all these reanalyses before 1975 (not shown). These biases prior to 1975 are consistent with considerable uncertainties in SSTs during this period, as well as a lack of sea ice observations in the Southern Ocean (Kennedy et al., 2011). Such uncertainties present a challenge for studying long-term temperature variation, e.g., analyses shown in Figures 10 and 11.

4 | CONCLUSIONS AND DISCUSSION

The newly digitized Signy synoptic temperature records compare well with those from Orcadas. Temperatures at both stations show a higher degree of variability in winter than summer. Signy is slightly warmer in summer and colder in winter. Signy temperatures demonstrate more variability than Orcadas with longer tails of extreme temperatures.

A statistically significant positive temperature trend (0.24 C·decade^{-1}) is detected in summer at Signy during 1947–1994 while no significant trend is detected in winter for both Signy and Orcadas Stations. The lack of winter warming trend in the SOIs differs from the strong winter warming trends observed in the western Antarctic Peninsula and South Shetlands Islands (Cannone et al., 2022; King et al., 2003; Royles et al., 2012). Results based on ERA5 reanalysis data suggest a strong linkage between the summer warming at Signy and warm anomalies on the eastern side of the Peninsula and an increase in the strength of the prevailing westerly winds, which has previously been attributed to circulation changes associated with stratospheric ozone depletion leading to a more positive SAM (Marshall, 2003; Thompson & Solomon, 2002).

In addition to these large-scale drivers, localized föhn winds may also play an important role in causing temperature variation and trends at the stations (Lu et al., 2023). For instance, here we show that Signy is significantly

warmer than Orcadas in summer and the effect increases with time along with the positive temperature trend during 1947–1994 (cf., Figure 8b). This warm trend is associated with enhanced northerlies and warmer SST anomalies upstream over the Brazil–Falkland Confluence (BFC) (cf., Figure 10). Signy Station is situated directly on the leeside of Coronation Island (cf., Figure 1), making the station more sensitive to föhn warming in the event of northerlies (King et al., 2017). Higher SSTs in summer over the BFC during 1972–1994 would allow more warm air to reach the SOIs via enhanced northerly winds (cf., Figure 10c). The effect is further amplified by föhn winds induced locally by Coronation Island. Conversely, Orcadas Station is situated on a low-lying isthmus joining parts of Laurie Island and east of Coronation Island, so does not receive the exceptionally warm föhn winds that affect Signy (King et al., 2017). These geographical differences between the two SOI stations may explain the greater warming trend at Signy and the observed temperature difference between Signy and Orcadas in summer (Lu et al., 2023).

Wintertime temperature in the SOIs is largely related to changes in regional sea-ice cover leading to increased heat fluxes between the open ocean surface and the overlying atmosphere (Simmonds et al., 2005). The important role of sea ice on regional Antarctic temperature has been noted previously (King et al., 2003; Reid et al., 2020; Turner et al., 2020; Weatherly et al., 1991). Similarly, here we have found that Orcadas temperatures are inversely related to SIC to the west of the SOIs on daily to monthly scales. In addition, there is a localized cooling trend along the narrow band on the east side of the Antarctic Peninsula in winter that is linked to the localized SST anomalies and a northward drift of sea ice from the Weddell Sea.

ERA5 temperatures are highly correlated with those at the stations even on synoptic timescales and agree exceedingly well with the station temperatures on monthly to annual timescales during the post-satellite period. However, ERA5 tends to underestimate extreme high temperatures in summer and overestimate extreme cold temperatures in winter. The underestimation is most likely due to a lack of representation of localized föhn effects, and the effect is more pronounced at Signy than Orcadas. The warm biases in winter are likely due to the rather crude representation of sea ice in the ERA5 assimilation model (King et al., 2022). ERA5 and other reanalysis datasets all underestimate station temperatures even for annual averages before 1979. These results reinforce the importance of using available historical station measurements when examining temperature variation in the sub-Antarctic islands, such as the SOIs.

AUTHOR CONTRIBUTIONS

Hua Lu: Conceptualization; methodology; software; data curation; investigation; formal analysis; writing – original draft; funding acquisition; supervision; writing – review and editing; project administration. **Steve Cowell:** Data curation; validation; project administration; supervision; resources; conceptualization. **John King:** Writing – review and editing; formal analysis; methodology; conceptualization; investigation; validation. **Andrew Orr:** Writing – review and editing; validation; investigation. **Tony Phillips:** Software; visualization; writing – review and editing; data curation; formal analysis; validation. **Emilia Dobb:** Formal analysis; data curation. **Jonathan Xue:** Data curation; software. **Sabina Kucieba:** Data curation. **Guy Phillips:** Data curation. **Gareth Marshall:** Writing – review and editing; validation.

ACKNOWLEDGEMENTS

This work is supported by core funding from the Natural Environment Research Council (NERC) to the British Antarctic Survey (BAS)'s Atmosphere, Ice and Climate Programme. Hua Lu, Andrew Orr and Gareth Marshall also received support from NERC National Capability International Grant SURface FluxEs In AnTarctica (NE/X009319/1). Andrew Orr is supported by the European Union's Horizon 2020 research and innovation framework programme under Grant 101003590 (PolarRES). Emilia Dobb, Jonathan Xue and Guy Phillips received funding from NERC Diversity, Equity and Inclusion Engagement Programme. We thank BAS archive team for assisting digitizing the Signy records and Laura Gerrish for help plotting Figure 1. Valuable comments made by Peter Convey on potential impact on Antarctic ecosystem and biodivercity are gratefully acknowledged. We are also grateful for the constructive comments by two anonymous referees that improved the original manuscript.

DATA AVAILABILITY STATEMENT

The Signy Station data are available from: Colwell and Lu (2023). The Orcadas Station data are available from the Data section under legacy.bas.ac.uk/met/READER/. ERA5 data were accessed from the Climate Data Store (CDS) provided by the Copernicus program. The monthly Sea Ice Concentrations from Nimbus-7 SMMR and DMSP SSM/I-SSMIS Passive Microwave Data, Version 2|National Snow and Ice Data Center (nsidc.org) are from nsidc.org/data/nsidc-0051/versions/2. Daily gridded Polar Pathfinder EASE-Grid Sea Ice Motion Version 4.1 data obtained from nsidc.org/data/nsidc-0116/versions/4. The monthly sea surface temperature (SST) data are obtained

from Hadley Centre at https://www.metoffice.gov.uk/hadobs/hadsst4/.

ORCID

Hua Lu https://orcid.org/0000-0001-9485-5082
John King https://orcid.org/0000-0003-3315-7568
Emilia Dobb https://orcid.org/0000-0002-8621-4370
Gareth Marshall https://orcid.org/0000-0001-8887-7314

REFERENCES

Alexander, L.V. & Arblaster, J.M. (2009) Assessing trends in observed and modelled climate extremes over Australia in relation to future projections. *International Journal of Climatology*, 29, 417–435. Available from: https://doi.org/10.1002/joc.1730

Alexander, M.J., Eckermann, S.D., Broutman, D. & Ma, J. (2009) Momentum flux estimates for South Georgia Island mountain waves in the stratosphere observed via satellite. *Geophysical Research Letters*, 36, L12816. Available from: https://doi.org/10.1029/2009GL038587

Ballerini, T., Hofmann, E.E., Ainley, D.G., Daly, K., Marrari, M., Ribic, C.A. et al. (2014) Productivity and linkages of the food web of the southern region of the western Antarctic Peninsula continental shelf. *Progress in Oceanography*, 122, 10–29. Available from: https://doi.org/10.1016/j.pocean.2013.11.007

Boisvert, L.N., Webster, M.A., Petty, A.A., Markus, T., Cullather, R.I. & Bromwich, D.H. (2020) Intercomparison of precipitation estimates over the Southern Ocean from atmospheric reanalyses. *Journal of Climate*, 33, 10627–10651. Available from: https://doi.org/10.1175/JCLI-D-20-0044.1

Bozkurt, D., Bromwich, D.H., Carrasco, J., Hines, K.M., Maureira, J.C. & Rondanelli, R. (2020) Recent near-surface temperature trends in the Antarctic Peninsula from observed, reanalysis and regional climate data. *Advances in Atmospheric Sciences*, 37, 477–493. Available from: https://doi.org/10.1007/s00376-020-9183-x

Cannone, N., Malfasi, F., Favero-Longo, S.E., Convey, P. & Guglielmin, M. (2022) Acceleration of climate warming and vascular plant expansion in maritime Antarctica. *Current Biology*, 32, 1–8. Available from: https://doi.org/10.1016/j.cub.2022.01.074

Chelton, D.B., Schlax, M.G., Freilich, M.H. & Milliff, R.F. (2004) Satellite measurements reveal persistent small-scale features in ocean winds. *Science*, 303, 978–983. Available from: https://doi.org/10.1126/science.1091901

Colwell, S. & Lu, H. (2023) Continuous subdaily meteorological records at Signy station, the South Orkney Islands 1947 - 1994 (Version 1.0) [Data set]. NERC EDS UK Polar Data Centre. https://doi.org/10.5285/d74b142c-7981-4a6a-9321-cf904a5668e6

Convey, P. & Peck, L.S. (2019) Antarctic environmental change and biological responses. *Science Advances*, 5, eaaz0888. Available from: https://doi.org/10.1126/sciadv.aaz0888

de Souza, M.M., Mathis, M. & Pohlmann, T. (2019) Driving mechanisms of the variability and long-term trend of the Brazil–Malvinas confluence during the 21st century. *Climate Dynamics*, 53, 6453–6468. Available from: https://doi.org/10.1007/s00382-019-04942-7

Gordon, A.L. (1989) Brazil-Malvinas Confluence-1984. *Deep Sea Research, Part A. Oceanographic Research Papers I*, 36, 359363–361384. Available from: https://doi.org/10.1016/0198-0149(89)90042-3

Harada, Y., Kamahori, H., Kobayashi, C., Endo, H., Kobayashi, S., Ota, Y. et al. (2016) The JRA-55 reanalysis: representation of atmospheric circulation and climate variability. *Journal of the Meteorological Society of Japan*, 94, 269–302.

Hersbach, H., Bell, B., Berrisford, P., Hirahara, S., Horányi, A., Muñoz-Sabater, J. et al. (2020) The ERA5 global reanalysis. *Quarterly Journal of the Royal Meteorological Society*, 146, 1999–2049. Available from: https://doi.org/10.1002/qj.3803

Hobbs, W.R., Klekociuk, A.R. & Pan, Y. (2020) Validation of reanalysis Southern Ocean atmosphere trends using sea ice data. *Atmospheric Chemistry and Physics*, 20, 14757–14768. Available from: https://doi.org/10.5194/acp-20-14757-2020

Hosking, J.S., Bannister, D., Orr, A., King, J.C., Young, E. & Phillips, T. (2014) Orographic forcing of surface winds over the shelf waters adjacent to South Georgia. *Atmospheric Science Letters*, 16, 50–55. Available from: https://doi.org/10.1002/asl2.519

Hoskins, B.J. & Hodges, K.I. (2005) A new perspective on Southern Hemisphere storm tracks. *Journal of Climate*, 18, 4108–4129. Available from: https://doi.org/10.1175/JCLI3570.1

Jones, P.D. (1995) Recent variations in mean temperature and the diurnal temperature range in the Antarctic. *Geophysical Research Letters*, 22, 1345–1348.

Jury, M.R. (2009) An intercomparison of observational, reanalysis, satellite, and coupled model data on mean rainfall in the Caribbean. *Journal of Hydrometeorology*, 10, 413–430. Available from: https://doi.org/10.1175/2008JHM1054.1

Kennedy, J.J., Rayner, N.A., Smith, R.O., Parker, D.E. & Saunby, M. (2011) Reassessing biases and other uncertainties in sea surface temperature observations measured in situ since 1850: 1. Measurement and sampling uncertainties. *Journal of Geophysical Research*, 116, D14103. Available from: https://doi.org/10.1029/2010JD015218

King, J.C., Bannister, D., Hosking, J.S. & Colwell, S.R. (2017) Causes of the Antarctic region record high temperature at Signy Island, 30th January 1982. *Atmospheric Science Letters*, 18, 491–496. Available from: https://doi.org/10.1002/asl.793

King, J.C., Marshall, G.J., Colwell, S.R., Arndt, S., Allen-Sader, C. & Phillips, T. (2022) The performance of the ERA-Interim and ERA5 atmospheric reanalyses over Weddell Sea pack ice. *Journal of Geophysical Research, Oceans*, 127, e2022JC018805. Available from: https://doi.org/10.1029/2022JC018805

King, J.C., Turner, J., Marshall, G.J., Connolley, W.M. & Lachlan-Cope, T.A. (2003) Antarctic Peninsula climate variability and its causes as revealed by analysis of instrumental records. In: Domack, E., Levente, A., Burnet, A., Bindschadler, R., Convey, P. & Kirby, M. (Eds.) *Antarctic peninsula climate variability: historical and paleoenvironmental perspectives*. Washington, DC: American Geophysical Union.

Li, X., Cai, W., Meehl, G.A., Meehl, G.A., Chen, D., Yuan, X. et al. (2021) Tropical teleconnection impacts on Antarctic climate changes. *Nature Reviews Earth and Environment*, 2, 680–698. Available from: https://doi.org/10.1038/s43017-021-00204-5

Lu, H., Orr, A., King, J.C., Phillips, T., Gilbert, E., Colwell, S.R. et al. (2023) Extreme warm events in the South Orkney Islands, Southern Ocean: compounding influence of atmospheric rivers and föhn conditions. *Quarterly Journal of the Royal Meteorological Society*, 1–24. https://doi.org/10.1002/qj.4578

Marshall, G.J. (2003) Trends in the Southern Annular Mode from observations and reanalyses. *Journal of Climate*, 16, 4134–4143. Available from: https://doi.org/10.1175/1520-0442

Marshall, G.J., Fogt, R.L., Turner, J. & Clem, K.R. (2022) Can current reanalyses accurately portray changes in Southern Annular Mode structure prior to 1979? *Climate Dynamics*, 59, 3717–3740. Available from: https://doi.org/10.1007/s00382-022-06292-3

Marshall, G.J. & Thompson, D.W.J. (2016) The signatures of large-scale patterns of atmospheric variability in Antarctic surface temperatures. *Journal of Geophysical Research: Atmospheres*, 121, 3276–3289. Available from: https://doi.org/10.1002/2015JD024665

Meredith, M.P., Meijers, A.S., Naveira Garabato, A.C., Brown, P.J., Venables, H.J., Abrahamsen, E.P. et al. (2015) Circulation, retention, and mixing of waters within the Weddell-Scotia Confluence, Southern Ocean: the role of stratified Taylor columns. *Journal of Geophysical Research, Oceans*, 120, 547–562. Available from: https://doi.org/10.1002/2014JC010462

Moline, M.A., Claustre, H., Frazer, T.K., Schofield, O. & Vernet, M. (2004) Alteration of the food web along the Antarctic Peninsula in response to a regional warming trend. *Global Change Biology*, 10, 1973–1980. Available from: https://doi.org/10.1111/j.1365-2486.2004.00825.x

Poli, P., Hersbach, H., Dee, D.P., Berrisford, P., Simmons, A.J., Vitart, F. et al. (2016) ERA-20C: an atmospheric reanalysis of the twentieth century. *Journal of Climate*, 29, 4083–4097. Available from: https://doi.org/10.1175/JCLI-D-15-0556.1

Reid, P.A., Stammerjohn, S., Massom, R.A., Barreira, S., Scambos, T. & Lieser, J.L. (2020) Sea ice extent, concentration, and seasonality [in "State of the climate in 2020"]. *Bulletin of the American Meteorological Society*, 101, S304–S306.

Rootes, D.M. (1988) The status of birds at Signy Island South Orkney Islands. *British Antarctic Survey Bulletin*, 80, 87–119.

Royles, J., Ogée, J., Wingate, L., Hodgson, D.A., Convey, P. & Griffiths, H. (2012) Carbon isotope evidence for recent climate-related enhancement of CO_2 assimilation and peat accumulation rates in Antarctica. *Global Change Biology*, 18, 3112–3124.

Simmonds, I., Rafter, A., Cowan, T., Watkins, A.B. & Keay, K. (2005) Large-scale vertical momentum, kinetic energy and moisture fluxes in the Antarctic sea-ice region. *Boundary-Layer Meteorology*, 117(1), 149–177.

Simmons, A.J. & Hollingsworth, A. (2002) Some aspects of the improvement in skill of numerical weather prediction. *Quarterly Journal of the Royal Meteorological Society*, 128, 647–677.

Slivinski, L.C., Compo, G.P., Whitaker, J.S., Sardeshmukh, P.D., Giese, B.S., McColl, C. et al. (2019) Towards a more reliable historical reanalysis: improvements for version 3 of the twentieth century reanalysis system. *Quarterly Journal of the Royal Meteorological Society*, 145, 2876–2908. Available from: https://doi.org/10.1002/qj.3598

Swart, N.C. & Fyfe, J.C. (2012) Observed and simulated changes in the Southern Hemisphere surface westerly wind-stress. *Geophysical Research Letters*, 39, L16711. Available from: https://doi.org/10.1029/2012gl052810

Thompson, D.W.J. & Solomon, S. (2002) Interpretation of recent Southern Hemisphere climate change. *Science*, 296, 895–899.

Turner, J. (2004) The El Niño–Southern Oscillation and Antarctica. *International Journal of Climatology*, 24, 1–31. Available from: https://doi.org/10.1002/joc.965

Turner, J., Colwell, S.R., Marshall, G.J., Lachlan-Cope, T.A., Carleton, A.M., Jones, P.D. et al. (2004) The SCAR READER project: towards a high-quality database of mean Antarctic meteorological observations. *Journal of Climate*, 17, 2890–2898.

Turner, J., Guarino, M.V., Arnatt, J., Jena, B., Marshall, G.J., Phillips, T. et al. (2020) Recent decrease of summer sea ice in the Weddell Sea, Antarctica. *Geophysical Research Letters*, 47, e2020GL087127. Available from: https://doi.org/10.1029/2020GL087127

Turner, J., Lu, H., King, J., Marshall, G.J., Phillips, T., Bannister, D. et al. (2021) Extreme temperatures in the Antarctic. *Journal of Climate*, 34, 2653–2668. Available from: https://doi.org/10.1175/JCLI-D-20-0538.1

Turner, J., Marshall, G.J., Clem, K., Colwell, S.R., Phillips, T. & Lu, H. (2019) Antarctic temperature variability and change from station data. *International Journal of Climatology*, 40, 2986–3007. Available from: https://doi.org/10.1002/joc.6378

Weatherly, J.W., Walsh, J.E. & Zwally, H.J. (1991) Antarctic sea ice variations and seasonal air temperature relationships. *Journal of Geophysical Research*, 96(C8), 15119–15130. Available from: https://doi.org/10.1029/91JC01432

Wille, J.D., Favier, V., Dufour, A., Gorodetskaya, I.V., Turner, J., Agosta, C. et al. (2019) West Antarctic surface melt triggered by atmospheric rivers. *Nature Geoscience*, 12, 911–916. Available from: https://doi.org/10.1038/s41561-019-0460-1

Yuan, X. (2004) High-wind-speed evaluation in the Southern Ocean. *Journal of Geophysical Research*, 109, D13101. Available from: https://doi.org/10.1029/2003JD004179

Zavialov, P.O., Waine, R.I. & Absy, J.M. (1999) Sea surface temperature variability off southern Brazil and Uruguay as revealed from historical data since 1854. *Journal of Geophysical Research, Oceans*, 104, 21021–21032. Available from: https://doi.org/10.1029/1998JC900096

Zazulie, N., Rusticucci, M. & Solomon, S. (2010) Changes in climate at high southern latitudes: a unique daily record at Orcadas spanning 1903–2008. *Journal of Climate*, 23, 189–196. Available from: https://doi.org/10.1175/2009JCLI3074.1

Zhu, J., Xie, A., Qin, X., Wang, Y., Xu, B. & Wang, Y. (2021) An assessment of ERA5 reanalysis for Antarctic near-surface air temperature. *Atmosphere*, 12, 217. Available from: https://doi.org/10.3390/atmos12020217

Zitto, M.E., Barrucand, M.G., Piotrkowski, R. & Canziani, P.O. (2016) 110 years of temperature observations at Orcadas Antarctic Station: multidecadal variability. *International Journal of Climatology*, 36, 809–823. Available from: https://doi.org/10.1002/joc.4384

How to cite this article: Lu, H., Cowell, S., King, J., Orr, A., Phillips, T., Dobb, E., Xue, J., Kucieba, S., Phillips, G., & Marshall, G. (2023). Temperature variation in the South Orkney Islands, maritime Antarctic. *International Journal of Climatology*, 1–18. https://doi.org/10.1002/joc.8302